Gene silencing reveals a specific function of hVps34 phosphatidylinositol 3-kinase in late versus early endosomes

Erin E. Johnson, Jean H. Overmeyer, William T. Gunning and William A. Maltese*

Department of Biochemistry and Cancer Biology, Medical University of Ohio, Toledo, OH 43614, USA

*Author for correspondence (e-mail: wmaltese@meduohio.edu)

Accepted 9 December 2005
Journal of Cell Science 119, 1219-1232 Published by The Company of Biologists 2006
doi:10.1242/jcs.02833

Summary

The human type III phosphatidylinositol 3-kinase, hVps34, converts phosphatidylinositol (PtdIns) to phosphatidylinositol 3-phosphate [PtdIns(3)*P*]. Studies using inhibitors of phosphatidylinositide 3-kinases have indicated that production of PtdIns(3)*P* is important for a variety of vesicle-mediated trafficking events, including endocytosis, sorting of receptors in multivesicular endosomes, and transport of lysosomal enzymes from the trans-Golgi network (TGN) to the endosomes and lysosomes. This study utilizes small interfering (si)RNA-mediated gene silencing to define the specific trafficking pathways in which hVps34 functions in human U-251 glioblastoma cells. Suppression of hVps34 expression reduced the cellular growth rate and caused a striking accumulation of large acidic phase-lucent vacuoles that contain lysosomal membrane proteins LAMP1 and LGP85. Analysis of these structures by electron microscopy suggests that they represent swollen late endosomes that have lost the capacity for inward vesiculation but retain the capacity to fuse with lysosomes. Morphological perturbation of the late endosome compartment was accompanied by a reduced rate of processing of the endosomal intermediate form of cathepsin D to the mature lysosomal form. There was also a reduction in the rate of epidermal growth factor receptor (EGFR) dephosphorylation and degradation following ligand stimulation, consistent with the retention of the EGFR on the limiting membranes of the enlarged late endosomes. By contrast, the suppression of hVps34 expression did not block trafficking of cathepsin D between the TGN and late endosomes, or endocytic uptake of fluid-phase markers, or association of a PtdIns(3)*P*-binding protein, EEA1, with early endosomes. LAMP1-positive vacuoles were depleted of PtdIns(3)*P* in the hVps34-knockdown cells, as judged by their inability to bind the PtdIns(3)*P* probe GFP-2xFYVE. By contrast, LAMP1-negative vesicles continued to bind GFP-2xFYVE in the knockdown cells.

Overall, these findings indicate that hVps34 plays a major role in generating PtdIns(3)*P* for internal vesicle formation in multivesicular/late endosomes. The findings also unexpectedly suggest that other wortmannin-sensitive kinases and/or polyphosphoinositide phosphatases may be able to compensate for the loss of hVps34 and maintain PtdIns(3)*P* levels required for vesicular trafficking in the early endocytic pathway or the TGN.

Key words: Endosome, Vps34, Phosphatidylinositol 3-kinase, Trafficking, Golgi, Lysosome

Introduction

Mammalian cells contain three distinct types of phosphoinositide 3-OH kinase (PI 3-kinase) (Fruman et al., 1998; Vanhaesebroeck et al., 2001). Type III PI 3-kinase catalyzes the phosphorylation of phosphatidylinositol at the D-3 position of the inositol ring, generating phosphatidylinositol 3-phosphate [PtdIns(3)*P*] (Odorizzi et al., 2000). The prototype for this type of enzyme, Vps34, was first identified in *Saccharomyces cerevisiae*, where it is one of several gene products required for delivery of soluble proteins to the vacuole (Schu et al., 1993; Herman et al., 1992) and for autophagic sequestration of cytoplasmic proteins during starvation (Kihara et al., 2001b; Wurmser and Emr, 2002). Under both circumstances, association of Vps34 with cellular membranes depends on a myristoylated regulatory subunit, Vps15 (Kihara et al., 2001b; Stack et al., 1995). In mammalian cells, Vps34 interacts with p150, a regulatory subunit similar to Vps15 (Panaretou et al., 1997).

PtdIns(3)*P* is required for membrane recruitment of several proteins implicated in the regulation of vesicular transport and intracellular protein sorting (Corvera, 2001; Simonsen et al., 2001). Some of these proteins (e.g. sorting nexins) contain a PX phosphoinositide-binding domain (Song et al., 2001; Cheever et al., 2001; Kanai et al., 2001; Xu et al., 2001), whereas others contain a structural motif termed the FYVE domain that binds to PtdIns(3)*P* with high affinity (Corvera et al., 1999; Fruman et al., 1999; Wurmser et al., 1999). Specific FYVE-domain proteins [early endosomal antigen 1 (EEA1), Rabenosyn-5, Rabip4] interact with Rab GTPases that control vesicle docking and fusion in the early endocytic pathway (Nielsen et al., 2000; Simonsen et al., 1998; Cormont et al., 2001; Kauppi et al., 2002). Interestingly, some Rabs that function in the early (Rab5) and late (Rab7) steps of the endocytic pathway also interact with the p150 subunit of the mammalian Vps34 complex, suggesting that the synthesis of PtdIns(3)*P* and the recruitment of FYVE-domain proteins

might be coordinately regulated (Murray et al., 2002; Stein et al., 2003).

Early evidence that PI 3-kinase activity is important for protein trafficking in mammalian cells came from studies in which inhibitors of PI 3-kinase (wortmannin and LY294002) were found to impair targeting of procathepsin D from the trans-Golgi network (TGN) to the lysosomal compartment (Davidson, 1995; Brown et al., 1995). Subsequent work using a kinase-deficient dominant-negative form of mammalian Vps34 suggested that the block in cathepsin D maturation was indeed related to a requirement for the type III PI 3-kinase (Row et al., 2001). Separate lines of evidence have suggested that mammalian Vps34 might also be required for receptor sorting in the early endocytic pathway. For example, Siddhanta et al. reported that microinjection of an inhibitory antibody against Vps34 interfered with ligand-stimulated translocation of the platelet-derived growth factor (PDGF) receptor between peripheral early endosomes and perinuclear late endosomal compartments (Siddhanta et al., 1998). Further investigations using inhibitory antibodies or wortmannin have suggested that Vps34 might play an essential role in the formation of internal vesicles within multivesicular endosomes (MVEs) (Futter et al., 2001), which are a key sorting compartment between early endosomes and lysosomes (reviewed by Gruenberg and Maxfield, 1995). Finally, in accord with studies in yeast, the mammalian Vps34 appears to play an important role in the process of macroautophagy in human cells subjected to nutrient deprivation (Petiot et al., 2000).

Although the aforementioned experimental approaches have provided important insights into the functions of Vps34 in mammalian cells, each has particular limitations. For example, wortmannin can simultaneously inhibit multiple types of PI 3-kinase (Vanhaesebroeck et al., 2001) and at least one type of phosphatidylinositol 4-kinase (Meyers and Cantley, 1997), making it difficult to attribute physiological effects to a specific enzyme. Likewise, overexpression of interfering Vps34 mutants may tie up key effectors or docking proteins that normally interact with more than one distinct kinase. Finally, antibody microinjection studies, although precise, can be applied only to small populations of cells, precluding most biochemical analyses of protein trafficking pathways. In recent years, the rapid development of methods for stable gene silencing by RNA interference (RNAi) has provided a powerful new option for defining the functions of specific proteins in mammalian cells (Sui et al., 2002; Paul et al., 2002; Brummelkamp et al., 2002).

In the present study, we have applied siRNA technology to pinpoint the function of human Vps34 (hVps34) in cultured U-251 glioblastoma cells. Suppression of hVps34 caused extreme swelling of late endosomes, consistent with defective membrane internalization into MVEs without concomitant reduction of incoming membrane traffic from the TGN and early endosomes. However, in contrast to some earlier findings based on PI 3-kinase inhibitors, specific silencing of hVps34 expression did not impair: (1) the exit of procathepsin D from the TGN; (2) the endocytic internalization of cell-surface receptors and fluid-phase markers; or (3) the association of a FYVE-domain protein (EEA1) with early endosomes. These studies indicate that the role of hVps34 in producing PtdIns(3)*P* for membrane trafficking is limited mainly to the multivesicular late endosome compartments, and that other mechanisms might exist to produce PtdIns(3)*P* required for vesicular trafficking in the early endosomes and TGN.

Results

Reduction of hVps34 expression by siRNA-mediated gene silencing causes accumulation of cytoplasmic vacuoles

To obtain a cell population in which expression of hVps34 was specifically and uniformly suppressed, we utilized a replication-deficient retroviral vector that drives the expression of RNAi sequences and confers puromycin resistance on infected cells (Brummelkamp et al., 2002). Vectors were engineered to contain either a sequence matching a unique

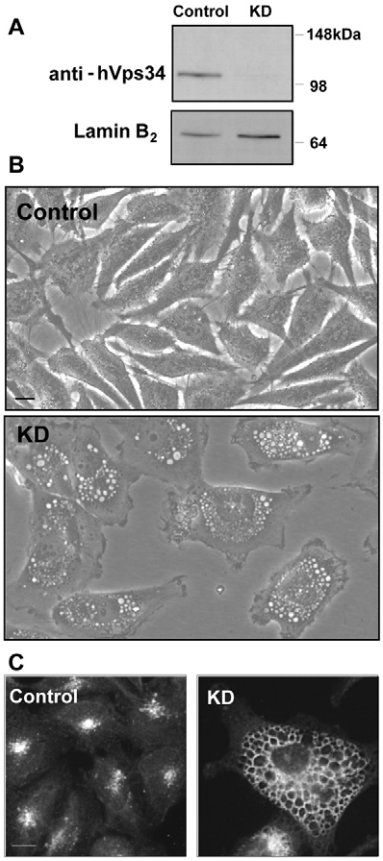

Fig. 1. siRNA-mediated suppression of hVps34 expression in U-251 glioma cells induces accumulation of LAMP1-positive cytoplasmic vacuoles. (A) U-251 cells infected with retrovirus carrying the control or hVps34 KD siRNA sequences surviving after 5 days of puromycin selection were subjected to immunoblot analysis with a polyclonal anti-hVps34 IgG as described in the Materials and Methods. Nuclear lamin B_2 served as one of several controls for nonspecific effects of the siRNA. (B) Phase contrast images of the live control and hVps34 KD cells. Bar, 10 μm. Based on counting 100 cells in multiple phase micrographs, 73% of the hVps34 KD cells exhibited the vacuolar phenotype, defined as multiple small-sized to intermediate-sized vacuoles (0.5-1.0 μ), with at least two vacuoles per cell exceeding a diameter of 2 μ. (C) Control and hVps34 KD cells were seeded at 100,000 cells/dish in 35 mm dishes. 24 hours later, cells were examined by immunofluorescence microscopy using a primary antibody against the lysosomal and late endosomal membrane protein LAMP1. Bar, 10 μm.

region of the hVPS34 mRNA, or a 'control' sequence that did not match any known GenBank entry. In preliminary tests with several cell lines infected with a green fluorescent protein (GFP) reporter construct, the human U-251 glioblastoma line showed high initial infection efficiency with the retroviral vector. Therefore, we chose to use this cell line for studies of hVps34. As illustrated by the immunoblots in Fig. 1A, expression of hVps34 was almost undetectable in puromycin-resistant cells that received the hVps34-'knockdown' vector (hVps34 KD cells), compared with cells that were infected with the control vector. In all of the experiments described in this paper, similar immunoblot results were obtained, verifying that expression of hVps34 was decreased by at least 90% relative to the parallel control cultures. Expression levels of unrelated proteins such as lamin B_2 (Fig. 1A), calreticulin and lactate dehydrogenase (LDH) (not shown) were comparable in the control and KD cells. The latter findings indicate that the loss of hVps34 expression was not due to a general effect of the siRNA on protein synthesis.

Examination of the cultures by phase contrast microscopy revealed striking morphological differences between the hVps34 KD cells and the matched controls (Fig. 1B). Specifically, more than 70% of the KD cells were filled with numerous phase-lucent spherical cytoplasmic vacuoles ranging 0.5-4.0 μ in diameter. To begin to assess the origin of the vacuoles in the hVps34 KD cells, we performed indirect immunofluorescence microscopy using an antibody against LAMP1, a glycoprotein localized in membranes surrounding lysosomes and late endosomes (Gough et al., 1999). As shown in Fig. 1C, the limiting membranes of the vacuoles in the KD cells were clearly outlined by antibodies against LAMP1.

To rule out the possibility that the striking accumulation of LAMP1-positive vacuoles induced by the siRNA targeted against hVps34 might be a result of off-target effects, we performed a similar study using a second retroviral construct containing an RNAi sequence matching a different non-overlapping portion of the hVPS34 mRNA. This construct, designated KD2, was similar to the original KD construct in being able to reduce the expression of hVps34 (Fig. 2A). Moreover, the phenotype of the cells expressing KD2 was similar to that described with the original KD construct, with accumulation of large LAMP1-positive vacuoles as a predominant feature (Fig. 2B). Therefore, for the remainder of the studies described in this report, we used the original KD construct with the understanding that its morphological and physiological effects were attributable to selective knockdown of hVps34 expression.

Electron microscopy revealed that the vacuoles in the hVps34 KD cells were generally electron lucent (Fig. 3A). Some contained sparsely distributed electron-dense material along with a few internal vesicles or membrane whorls (Fig. 3B). The vacuoles were always circumscribed by a single membrane, indicating that they did not represent enlarged autophagosomes (Fig. 3B).

Vacuoles in hVps34 KD cells are derived from late endosomes

Previous reports have suggested that hVps34 is associated with Golgi membranes (Kihara et al., 2001a) and endosomes (Murray et al., 2002) in mammalian cells. The immunofluorescent localization of LAMP1 to the vacuole membranes (Figs 1 and 2) is most consistent with a late endosomal origin for these structures. To explore this possibility further, we performed indirect immunofluorescence microscopy using several additional antibodies against proteins localized in specific organelles (Fig. 4). The limiting membranes of the vacuoles were clearly outlined by an antibody against another lysosomal/late endosomal membrane glycoprotein, LGP85 (Kuronita et al., 2002). An antibody

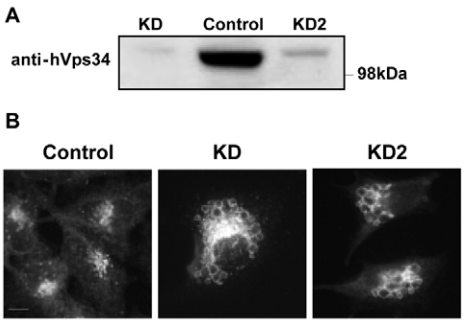

Fig. 2. Accumulation of LAMP1-positive vacuoles is specific to suppression of hVps34 expression. (A) U-251 cells infected with retrovirus harboring the control or two different hVps34-specific RNAi sequences (KD and KD2) were subjected to immunoblot analysis as described previously. (B) Control, hVps34 KD and hVps34 KD2 cells were seeded at 100,000 cells/dish in 35 mm dishes. 48 hours later, cells were examined by immunofluorescence microscopy using an antibody against LAMP1. Bar, 10 μm.

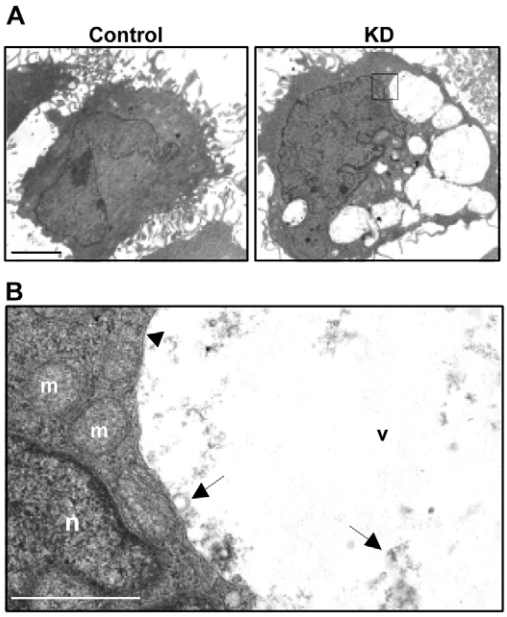

Fig. 3. Vacuoles in the hVps34 KD cells are membrane-bound structures with occasional internal vesicles and electron-dense material. Control and hVps34 KD cells were examined by electron microscopy. (A) Control and KD cells magnified 3,900×. Bar, 5 μm. (B) Highlighted region of KD cell from panel A at 21,000×. Bar, 1 μm. Labeled structures: m, mitochondria; n, nucleus; v, vacuole. The arrowhead points to a single membrane surrounding the vacuole. Arrows point to occasional small internal vesicles and electron-dense material.

against lysobisphosphatidic acid (LBPA), a phospholipid that is normally concentrated in the internal membranes of MVEs and late endosomes (Kobayashi et al., 1998), did not stain the interior of the vacuoles and reacted with the peripheral membranes with less uniformity than the LAMP1 and LGP85 antibodies. In the control cells, LAMP1, LGP85 and LBPA were all localized to clusters of punctuate structures adjacent to the nucleus, typical of the late endosome and/or lysosome distribution of these markers seen in many types of cells.

Immunofluorescent staining for proteins associated with membranes of the Golgi apparatus or endoplasmic reticulum suggested that the vacuoles did not arise directly from these compartments in the hVps34 KD cells (Fig. 4). The Golgi marker GM130 exhibited a compact juxtanuclear distribution typical of Golgi localization. The cation-independent mannose-6-phosphate receptor (M6PR) did not accumulate in the limiting membranes of the vacuoles. Instead, M6PR was detected mainly in a compact region adjacent to the nucleus, similar to the GM130 Golgi marker. The M6PR is involved in the delivery of newly synthesized lysosomal hydrolases from the TGN to MVEs (Le Borgne and Hoflack, 1998; Ghosh et al., 2003; Press et al., 1998). The distribution of M6PR in the control and hVps34 KD cells is consistent with previous reports indicating that, at steady state, most of the M6PR is localized in the TGN (Hirst et al., 1998; Kobayashi et al., 1998). Calreticulin exhibited a diffuse web-like pattern that appeared to be concentrated in regions of the cytoplasmic compartment displaced by the vacuoles. Although this gives the appearance that the vacuoles are surrounded by calreticulin, we do not believe that calreticulin is actually in the limiting

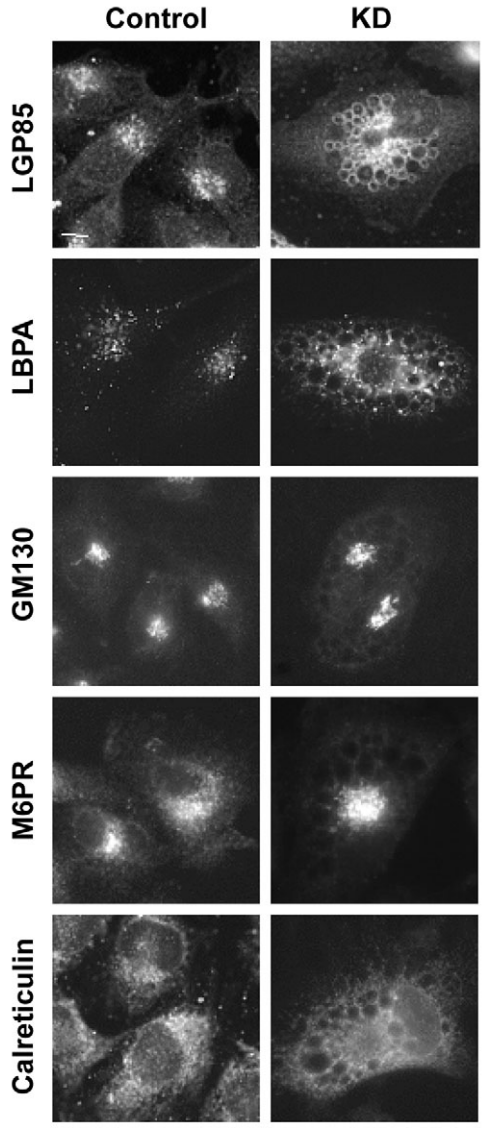

Fig. 4. Vacuoles in the hVps34 KD cells exhibit characteristics of late endosomes or lysosomes. Control and hVps34 KD cells were seeded at 100,000 cells/dish in 35 mm dishes. 24 hours later, cells were examined by immunofluorescence microscopy using the primary antibodies indicated at the left of the figure. Bar, 10 μm.

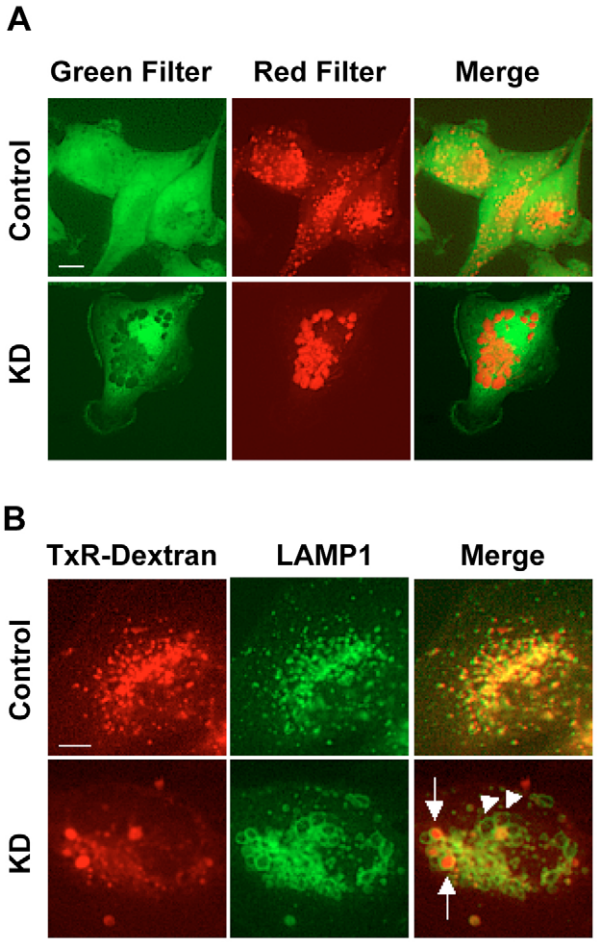

Fig. 5. Vacuoles in the hVps34 KD cells are acidic and receive traffic from the endocytic compartment. (A) Control and hVps34 KD cells were incubated with 2.5 μg/ml Acridine Orange (AO) for 30 minutes. The cells were then examined by fluorescence microscopy using green (excitation wavelength: 465-495 nm; emission wavelength: 515-555 nm) and red (excitation wavelength: 528-553 nm; emission wavelength 600-660 nm) filters. Red fluorescence emanates from AO in acidic compartments. Bar, 10 μm. (B) Control and KD cells were incubated with 500 μg/ml Texas Red (TxR)-dextran for 16 hours. Following incubation for 2 hours, cells were fixed and co-stained with a monoclonal antibody against LAMP1. Arrows indicate vacuoles containing both LAMP1 and TxR-dextran. Arrowheads point to vacuoles lacking TxR-dextran. Bar, 10 μm.

membrane, based on a comparison with the more obvious membrane staining of LAMP1 and LGP85. Nevertheless, at the level of resolution afforded by light microscopy, we cannot definitively rule out some association of calreticulin with the vacuoles.

To characterize the cytoplasmic vacuoles further, we performed supravital staining of the cells with the lysosomotropic agent Acridine Orange (AO) (Fig. 5A). The non-protonated monomeric form of AO emits green fluorescence in the cytoplasm. However, when the dye enters an acidic compartment (e.g. lysosomes or late endosomes), the protonated form becomes trapped in aggregates that fluoresce bright red or orange (Traganos and Darzynkiewicz, 1994; Paglin et al., 2001; Kanzawa et al., 2003). The images in Fig. 5A demonstrate that the numerous vacuoles observed in the hVps34 KD cells are acidic vesicular organelles that sequester AO.

On the basis of the presence of lysosomal membrane markers and their ability to sequester AO, we hypothesized that the vacuoles in the hVps34 KD cells were derived from late endosomes or lysosomes. To test this hypothesis further, we labeled the endosomal system by adding a fluid phase tracer, Texas Red (TxR)-dextran, to the culture medium for 16 hours (Fig. 5B). The distribution of TxR-dextran was compared with that of LAMP1. In the control cells, the TxR-dextran was concentrated in a cluster of small vesicles adjacent to the nucleus. Consistent with the expected uptake of TxR-dextran into endosomes and lysosomes, the tracer showed extensive colocalization with LAMP1-positive compartments (Fig. 5B). Examination of the hVps34 KD cells revealed that the fluid phase tracer was incorporated into some of the large LAMP1-positive cytoplasmic vacuoles (arrows) as well as numerous smaller vesicular structures (Fig. 5B). However, the persistence of some LAMP1-positive vacuoles that did not incorporate TxR-dextran after prolonged incubation (arrowheads) suggests that a subpopulation of these structures might be functionally disengaged from the fluid-phase endocytic pathway.

Suppression of hVps34 expression does not disrupt the PtdIns(3)*P*-dependent localization of the early endosome protein EEA1

To assess the morphology of the early endosomes, we examined the subcellular distribution of EEA1, a FYVE-domain protein that is known to be recruited to the early endosome membrane in a PtdIns(3)*P*- and Rab5-dependent manner (Christoforidis et al., 1999; Simonsen et al., 1998). There was no clear association of EEA1 with the membranes of the numerous large vacuoles in the hVps34 KD cells (Fig. 6A). Instead, the protein was detected predominantly in a population of smaller vesicles with a pattern similar to the control cells. We occasionally observed ring-like structures that could represent swollen early endosomes in the KD cells. However, these structures were not numerous and were distinct from the much larger phase-lucent vacuoles. In contrast to the bright punctate fluorescence pattern of EEA1 in the control and hVps34 KD cells, control cells treated with 1 μM wortmannin showed only a diffuse reticular staining pattern. The loss of punctate EEA1 distribution is consistent with the release of EEA1 from endosomal membranes reported to occur in other cell lines treated with PI 3-kinase inhibitors (Simonsen et al., 1998; Petiot et al., 2003). At 1 μM, wortmannin generally

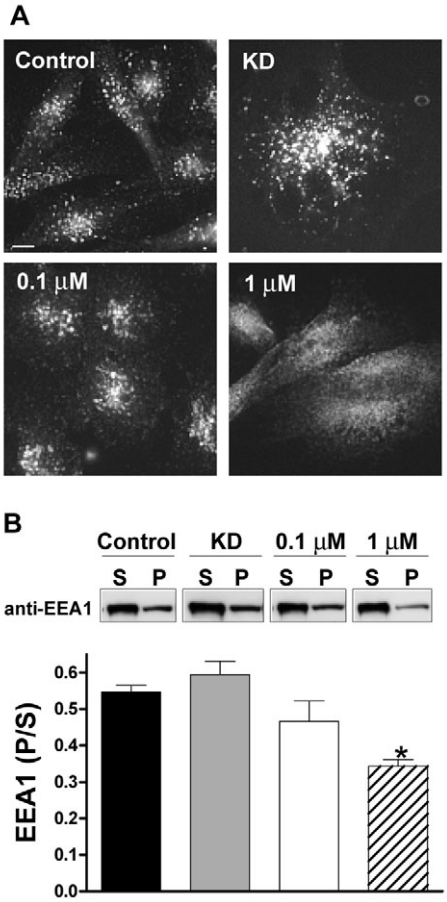

Fig. 6. Suppression of hVps34 expression does not prevent membrane association of the early endosome marker EEA1. (A) Control and hVps34 KD cells were seeded at 100,000 cells/dish in 35 mm dishes. 24 hours later, cells were examined by immunofluorescence microscopy using an anti-EEA1 antibody. Control cells treated with 0.1 μM or 1 μM wortmannin for 1 hour are also shown. (B) Cytosol (S) and particulate (P) fractions were prepared from control cells, hVps34 KD cells, or control cells treated for 1 hour with the indicated concentrations of wortmannin (0.1 μM or 1 μM), as described in the Materials and Methods. Immunoblot analysis was performed with an antibody against EEA1 and the relative amount of EEA1 recovered in the P fraction is expressed as a ratio to the amount in the S fraction. The results are means (±s.e.m.) of three determinations performed on separate cultures. The asterisk indicates that the decrease relative to the control and KD cells was significant at $P< 0.05$ (Student's *t* test). Essentially the same results were obtained when the amount of EEA1 recovered in the P fraction was normalized to the amount of a membrane marker (calreticulin) recovered in the same fraction (not shown).

inhibits all types of PI 3-kinase (Vanhaesebroeck et al., 2001). Interestingly, a lower concentration of wortmannin (0.1 μM), which is reported to inhibit type I and type III PI 3-kinases but not the type II PI 3-kinase isoform C2α (Virbasius et al., 1996; Prior and Clague, 1999), did not disrupt EEA1 localization in the U-251 cells (Fig. 6A).

To examine the subcellular distribution of EEA1 further, control and hVps34 KD cells were fractionated into cytosolic and particulate components, and the partitioning of EEA1 between these components was determined by immunoblot

analysis (Fig. 6B). The proportion of EEA1 in the particulate versus soluble fraction in the KD cells was not significantly different from the controls. When considered together with the immunofluorescence studies in Fig. 6A, these results indicate that EEA1 is able to associate with endosomal membranes in U-251 cells under conditions where expression of hVps34 is almost completely suppressed. Short-term treatment of the cells with 1 μM wortmannin resulted in a significant ($P<0.05$) decline in the proportion of EEA1 in the particulate fraction compared with either the control or KD cells (Fig. 6B). This decrease paralleled the elimination of punctate EEA1 fluorescence in Fig. 6A, suggesting that it corresponds to the loss of EEA1 from endosomal membranes. By contrast, 0.1 μM wortmannin produced only a slight and statistically insignificant decline in the ratio of particulate to soluble EEA1 (Fig. 6B), in accord with the persistence of punctate EEA1 staining at the lower wortmannin concentration (Fig. 6A). The latter observation suggests that the lack of an effect of hVps34 knockdown on EEA1 membrane localization could be related in part to a type II PI 3-kinase contributing to the maintenance of the PtdIns(3)*P* pool in the early endosomes.

LAMP1-positive vacuoles are depleted of PtdIns(3)*P*, as measured by a GFP-2xFYVE probe

The preceding observations predict that LAMP1-positive late endosome compartments are depleted of PtdIns(3)*P* in the hVps34 KD cells, whereas early endosome compartments are at least partially spared. To test this hypothesis, we transfected control and hVps34 KD cells with a vector that expresses a GFP-2xFYVE probe previously shown to bind specifically to PtdIns(3)*P* in cellular membranes (Gillooly et al., 2003; Gillooly et al., 2000; Petiot et al., 2003). GFP-2xFYVE was localized in numerous cytoplasmic vesicles in the control cells (Fig. 7, upper panels). Some of these were positive for LAMP1, whereas others were not, consistent with the presence of PtdIns(3)*P* in both early and late endosomes. Most of the vesicles labeled with GFP-2xFYVE in the control cells (Fig. 7) appeared swollen when compared with normal endosomes (e.g. Fig. 6A control). This was expected, given earlier reports

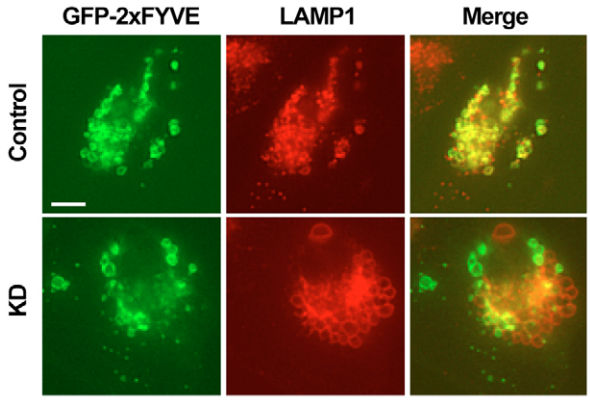

Fig. 7. LAMP1-positive vacuoles formed in hVps34 KD cells are depleted of PtdIns(3)*P*, as measured by localization of a GFP-2xFYVE probe. Control or hVps34 KD cells were transfected with a vector encoding GFP-2xFYVE. After 16 hours, the cells were processed for immunofluorescence, using primary antibodies against GFP and LAMP1. Bar, 10 μm.

that overexpression of 2xFYVE probes can disrupt early endosome fusion (Gillooly et al., 2000) and sorting in MVEs (Petiot et al., 2003). The presence of PtdIns(3)*P* in LAMP1-positive compartments might seem surprising in light of the aforementioned evidence that PtdIns(3)*P* is localized predominantly in early endosomes. However, some studies have also shown that the GFP-2xFYVE probe localizes extensively on Rab7-positive late endosomes (Stein et al., 2003), which are typically positive for LAMP1 (Bucci et al., 2000). In contrast to the control cells, a very different picture emerged when the hVps34 KD cells were examined by the same technique (Fig. 7, lower panels). Here, the numerous large LAMP1-positive vesicles did not bind the GFP-2xFYVE probe, suggesting that they are indeed derived from late endosomes depleted of PtdIns(3)*P*. However, the hVps34 KD cells continued to exhibit GFP-2xFYVE labeling of a distinct population of LAMP1-negative vesicles (Fig. 7). We presume that these vesicles are early endosomes that are not completely depleted of PtdIns(3)*P*, although we are unable to confirm this directly by EEA1 localization because the 2xFYVE probe releases EEA1 from membranes (Petiot et al., 2003).

Endocytosis is not disrupted in hVps34 KD cells

The earlier observation that a fluid-phase tracer, TxR-dextran, was incorporated into LAMP1-positive compartments in the hVps34 KD cells (Fig. 5B) suggested that production of PtdIns(3)*P* by hVps34 was not essential for delivery of early endosome cargo to late endosomes in U-251 cells. Previous studies have shown that, when vesicular transport from early endosomes to late endosomes is inhibited, there is a reduction in cellular uptake of the soluble endocytic tracer horseradish peroxidase (HRP) (Li and Stahl, 1993; Mayran et al., 2003). Thus, to explore the integrity of the early endocytic pathway in the hVps34 KD cells, we determined the kinetics of HRP uptake. As shown in Fig. 8A, the rate of HRP uptake was not reduced in the KD cells. On the contrary, HRP uptake was increased compared with the controls. One possible explanation for this observation might be an increased intracellular sequestration of HRP due to a defect in endosome recycling in the hVps34 KD cells. To address this possibility, cells were pre-loaded with biotinylated transferrin and the amount of ligand released into the medium was measured during a chase with unlabeled transferrin. As shown in Fig. 8B (inset), an increased amount of biotinylated transferrin was taken up into the hVps34 KD cells compared with the controls during the initial 30 minute pre-loading period, consistent with the increased HRP uptake observed in Fig. 8A. However, the percentages of intracellular biotinylated transferrin subsequently released into the medium were essentially identical for the control and KD cells (Fig. 8B). These results indicate that endosome recycling is not disrupted in the hVps34 KD cells. It remains to be determined what factors may contribute to the apparent increase in endocytic uptake of the fluid-phase marker and transferrin in the hVps34 KD cells.

As a means to evaluate growth factor receptor trafficking in the endocytic pathway, we examined the fate of activated epidermal growth factor receptor (EGFR). In serum-deprived cells grown in the absence of EGF, degradation of EGFR is minimal and receptors accumulate on the cell surface. However, upon addition of EGF, the receptors are rapidly activated by tyrosine phosphorylation in the C-terminal

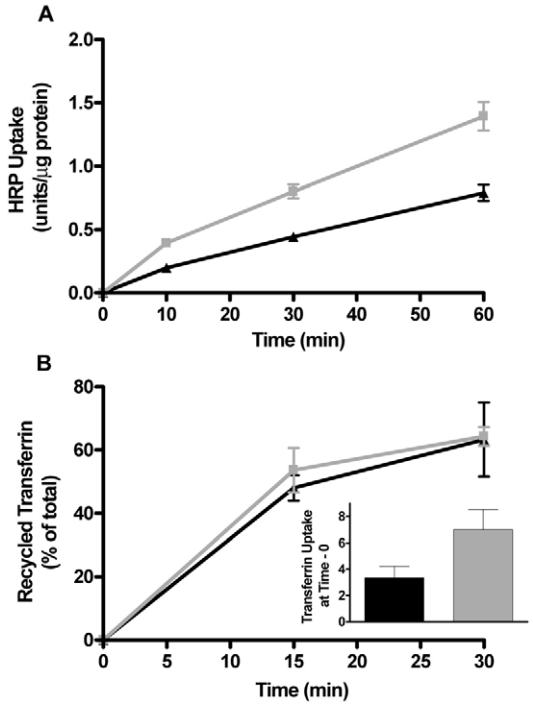

Fig. 8. (A) Suppression of hVps34 expression does not interfere with the endocytosis of a fluid phase marker, horseradish peroxidase (HRP). (A) Control (black) and hVps34 KD (gray) cells were incubated for the indicated periods of time with 2 mg/ml HRP in DMEM + 1% BSA. Washed cells were lysed and HRP activity was determined as described in the Materials and Methods. Each point represents the mean±s.e.m. from triplicate dishes of each cell line. (B) Suppression of hVps34 expression does not impair recycling of transferrin. Control (black) and hVps34 KD (gray) cells were allowed to internalize biotinylated transferrin for 30 minutes, then were chased with an excess of unlabeled transferrin for 15 or 30 minutes. The amounts of biotinylated transferrin in the cells and medium were determined as described in the Materials and Methods. The recycled transferrin (released into the medium) is expressed as percentage of total biotinylated transferrin. The bar graph in the inset shows the relative amount of biotinylated transferrin (normalized to calreticulin) taken up by the control (black bar) and KD (gray bar) cells after the 30 minutes pre-loading period. Each point represents the mean±s.e.m. from triplicate dishes of each cell line.

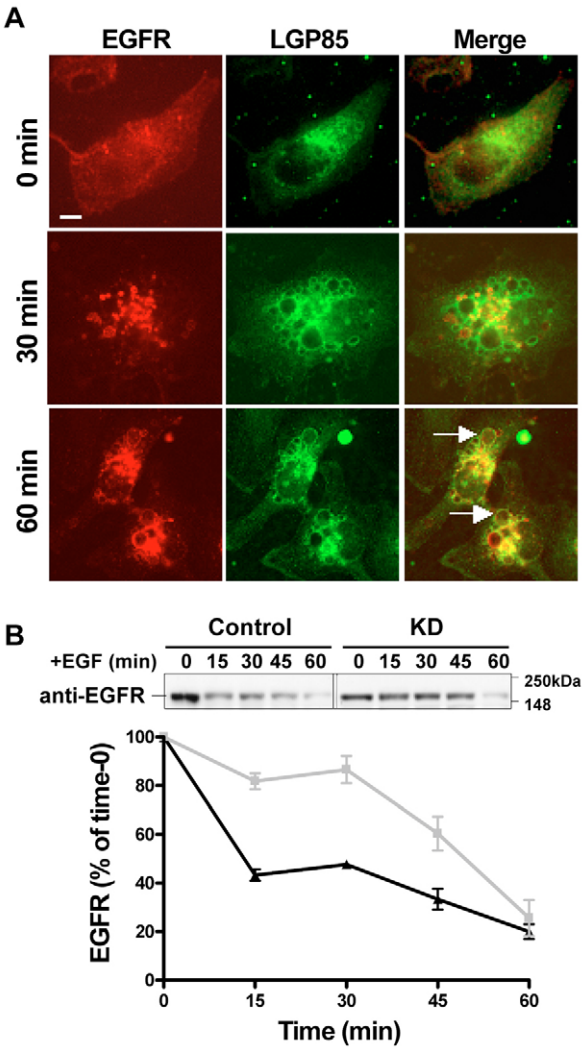

Fig. 9. Suppression of hVps34 expression does not impede internalization of the EGFR, but slows initial receptor degradation. Control and hVps34 KD cells were stimulated with EGF after overnight incubation with serum-free medium. (A) KD cells were fixed and co-stained with EGFR and LGP85 antibodies before addition of EGF (0 min) and at different time points (30 min, 60 min) after addition of EGF. Arrows indicate vacuoles positive for both the EGFR and LGP85. The brightness of the EGFR image at 60 minutes was enhanced by approximately 50% to compensate for its weaker EGFR immunofluorescence compared with the brightness of the image at 30 minutes. Bar, 10 μm. (B) To measure EGFR degradation, triplicate cultures of control and KD cells were harvested at the indicated times after the addition of EGF and subjected to immunoblot analysis for total EGFR. The graph illustrates the data (mean±s.e.m.) generated from densitometer scans of ECL signals on film.

cytoplasmic domain and the EGF-EGFR complexes are internalized into clathrin-coated early endosomes. Downregulation of activated receptors depends upon their delivery to MVEs, where receptor complexes are sorted into internal vesicles that are ultimately degraded when late endosomes fuse with lysosomes (Katzmann et al., 2002). When EGFR was localized by immunofluorescence, 30 minutes after addition of EGF to hVps34 KD cells, most of the receptors were found in small internal vesicles that were distinct from the large vacuoles labeled by the late endosome/lysosome marker LGP85 (Fig. 9A). However, after 60 minutes, some EGFR could be detected in the limiting membranes surrounding the large LGP85-positive vacuoles (Fig. 9A, arrows). This suggested that delivery of EGFR from early endosomes to the surface membranes of the enlarged late endosomal structures was not impaired in the hVps34 KD cells.

Knockdown of hVps34 impairs degradation of the EGFR

To examine degradation of the EGFR, immunoblot analysis of total EGFR was performed at intervals after addition of EGF. The results indicate that the initial rate of degradation of the receptor was substantially slowed in the hVps34 KD cells compared with the controls (Fig. 9B); however, between 45-60 minutes, the receptor eventually underwent degradation to an extent similar to the controls. Although the portion of the blot

shown in the figure focuses on the full-length receptor, examination of the lower portion of the blot did not reveal any evidence for accumulation of unique partially degraded EGFR fragments in the KD cells.

To assess the amount of activated EGFR at intervals after EGF stimulation, blots were probed with an antibody that specifically recognizes phosphorylated residue Tyr1068 in the C-terminal domain of the receptor, then re-probed to quantify total EGFR. The C-terminal domain faces the cytoplasm when EGFR is in the limiting membrane of the endosome, but it is incorporated into the lumen of vesicles that invaginate to the interior of the MVE (Katzmann et al., 2002). As shown in Fig. 10A, nearly all of the EGFR was in the non-phosphorylated state at the starting point; but, within 30 minutes of adding EGF, both control and hVps34 KD cells exhibited a dramatic increase in the proportion of phospho-EGFR relative to total receptor. However, in the hVps34 KD cells, the ratio of phospho-EGFR to total EGFR was approximately double that observed in the control cells. Thus, it appears that, prior to being exposed to lysosomal proteases, a higher percentage of the EGFR remains phosphorylated in the hVps34 KD cells. In agreement with this concept, activation of the ERK (p44/42 MAP kinase) signaling pathway, as measured by the ratio of phospho-ERK1/2 to total ERK1/2, was augmented in the hVps34 KD cells compared with the controls (Fig. 10B).

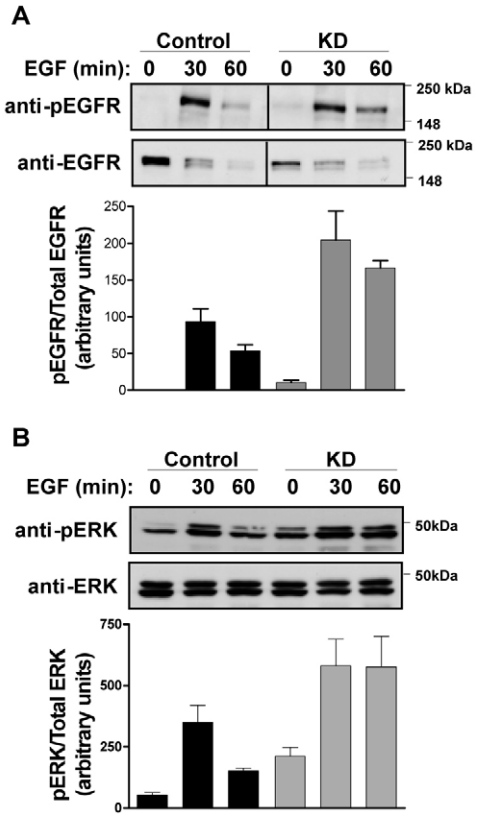

Fig. 10. Suppression of hVps34 expression potentiates EGFR signaling. To measure EGFR phosphorylation and signaling, the control and KD cells were harvested at the indicated times after the addition of EGF and subjected to immunoblot analysis for (A) phospho-EGFR (pEGFR) and total EGFR, or (B) phospho-ERK1/2 (pERK) and total ERK1/2. The bar graphs illustrate the data generated from Kodak Imager scans of blots from triplicate cultures of each cell line.

Knockdown of hVps34 does not impair transport of procathepsin D from the TGN to endosomes, but slows cathesin D processing in lysosomes

To determine if the enlarged endosomal structures in the hVps34 KD cells were capable of accepting cargo normally delivered to late endosomes from the TGN, we focused on the lysosomal enzyme cathepsin D (Pohlmann et al., 1995). Newly synthesized procathepsin D (51-53 kDa) associates with the cation-independent M6PR in the TGN and is delivered to the endosomal compartment, where it is activated by removal of the propeptide to generate an intermediate that migrates at 46-48 kDa on SDS gels. The final step in cathepsin D processing is completed in the lysosomes, where the intermediate is cleaved to the mature form, which contains two non-covalently linked chains of 31 kDa and 14 kDa (Rijnboutt et al., 1992; Delbruck et al., 1994).

To evaluate the processing of newly synthesized procathepsin D, we performed a pulse-chase analysis (Fig. 11A). When [^{35}S]methionine-labeled cathepsin D was immunoprecipitated after a 30 minute pulse, nearly all of the radiolabeled protein was in the 53 kDa form in both control and KD cells. After a 4 hour chase, the control cells converted most of the procathepsin D to the mature form, with some intermediate form still detected. There was no residual radiolabeled procathepsin D in the hVps34 KD cells after the 4 hour chase, suggesting that delivery of procathepsin D from the TGN to the late endosome compartment was not substantially altered in the absence of hVps34 (Fig. 11A). However, compared with the control, there was a 50% decrease in the relative amount of the mature 31 kDa cathepsin D and a corresponding increase in the 47 kDa intermediate form in the KD cells (Fig. 11A). By contrast, a complete block of cathepsin D maturation instituted by raising the endosomal and lysosomal pH with NH_4Cl, is manifested by the absence of any radiolabeled 31 kDa cathepsin D after a 4 hour chase (Fig. 11A). These results are indicative of a kinetic block at the late endosome to lysosome transition in the hVps34 KD cells, resulting in slower lysosomal processing of the cathepsin D intermediate, but not a complete obstruction of its delivery to lysosomes.

This interpretation is reinforced by the immunoblot depicted in Fig. 11B, which shows that the steady-state level of the 47 kDa cathepsin D intermediate was markedly elevated in the hVps34 KD cells. In agreement with the pulse-chase study, there was no accumulation of the 53 kDa procathepsin D that could indicate a problem with trafficking from the TGN. Likewise, immunoblot analysis of procathepsin D released into the medium showed no indication that an increased amount of procathepsin D was being diverted into the secretory pathway in the hVps34 KD cultures (not shown). The similar levels of mature 31 kDa cathepsin D in the immunoblots of control and KD cells might seem puzzling at first, given the slower intermediate processing observed in Fig. 11A. However, this is most probably related to the fact that lysosomal enzymes have long half-lifes compared with their precursors (Hentze et al., 1984; Reilly, et al., 1989; Nissler et al., 1999); thus, over time, a reduced rate of intermediate processing might have an

imperceptible impact on the accumulated pool of end product detected by immunoblot assay.

Vacuoles in the hVps34 KD cells can merge with pre-existing lysosomes

The finding that final proteolytic processing of the 47 kDa cathepsin D intermediate was slowed but not completely blocked in the hVps34 KD cells strongly suggests that the enlarged endosome-derived vacuoles are able to acquire lysosomal characteristics by limited fusion with pre-existing lysosomes. This could also explain how EGFR is ultimately degraded in the hVps34 KD cells (Fig. 9B). Further support for this interpretation comes from an examination of the hVps34 KD cells by immunogold electron microscopy, using a primary antibody against cathepsin D to identify lysosomes (Fig. 11C). With this method, we frequently noted smaller electron-dense lysosomes, heavily labeled with gold particles, in close proximity to the larger electron-lucent vacuoles (Fig. 11C, arrow). In some cases, it appeared that cathepsin D was being delivered to the lumen of the vacuole after fusion with the structure (Fig. 11C, black arrowhead). When taken together with the results of the cathepsin D processing studies (Fig. 11A,B) and the EGFR degradation experiment (Fig. 9B), these morphological observations indicate that the enlarged endosome-derived vacuoles in the hVps34 KD cells retain a limited capacity to fuse with lysosomal compartments.

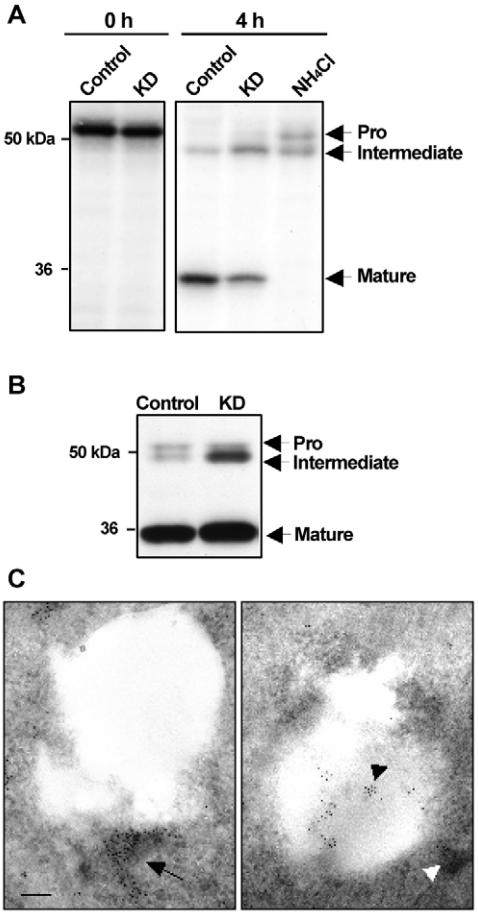

Fig. 11. The late endosomal intermediate form of cathepsin D accumulates in the absence of hVps34, but there is no inhibition of the early step of procathepsin D processing. (A) Control and hVps34 KD cells were seeded at 350,000 cells/dish in 10 cm dishes. Cells were labeled with 100 μCi/ml [^{35}S]methionine, then harvested after 30 minutes or chased in medium with unlabeled methionine for 4 hours. A separate control culture was incubated with 15 mM NH_4Cl during the 4 hour chase. Cathepsin D was immunoprecipitated and subjected to SDS-PAGE and fluorography. Pro, newly synthesized 51-53 kDa procathepsin D containing a propeptide; Intermediate, cathepsin D after removal of the propeptide to generate an intermediate form that migrates at 46-48 kDa; Mature, cathepsin D after cleavage to generate the mature form that contains two non-covalently linked chains of 31 kDa and 14 kDa. (B) Immunoblot analysis of endogenous cathepsin D in whole cell lysates from control and hVps34 KD cells. (C) The hVps34 KD cells were subjected to immunogold labeling with an antibody against cathepsin D. The left panel shows a lysosome heavily labeled for cathepsin D (arrow) adjacent to a larger electron-lucent vacuole. The right panel shows cathepsin D delivered to the lumen of an enlarged vacuole (black arrowhead), with a lysosome adjacent to the vacuole (white arrowhead). Bar, 0.5 μm.

Suppression of hVps34 expression inhibits cell proliferation

The cells in the hVps34 KD cultures were approximately 2-3 times larger than those in the control cultures, and they did not reach a comparable density when maintained for several days after the initial puromycin selection. This prompted us to ask whether suppressing the expression of hVps34 might affect the growth of the U-251 cells. As shown in Fig. 12A, the growth rate of the KD cells was markedly reduced compared with the matched control cell line. A decreased rate of cell proliferation was confirmed by comparing the incorporation of [methyl-^{3}H]thymidine into DNA in control versus KD cells at points where the control cells were at low density (day 2) or near confluence (day 6) (Fig. 12B). Apoptotic cell death, measured by annexin staining, was not a major factor in reducing the density of hVps34 KD cells, even though U-251 cells were capable of a robust apoptotic response when treated with tumor necrosis factor α (TNF-α) (Fig. 12C).

Discussion

In the present study, we used the highly specific method of siRNA-mediated gene silencing to explore the function of the human type III PI 3-kinase hVps34. Our observations indicate that silencing of hVps34 expression mainly affects membrane-sorting events within the multivesicular and late endosome compartments, with surprisingly little effect on vesicular trafficking through the early part of the endocytic pathway or the export of proteins from the TGN to endosomes. The acidic characteristics of the vacuoles in the hVps34 KD cells, coupled with the dearth of internal structures and the presence of LAMP1 and LGP85 in their limiting membranes, indicates that they represent enlarged late endosomes. Interestingly, despite their distorted size, these structures seem to retain a substantial capacity to merge with primary lysosomes, allowing for eventual degradation of the EGFR and only partial impairment of the processing of the intermediate form of cathepsin D to the mature form.

One of the novel findings emerging from the present studies is the absence of any effect of blocking hVps34 expression on the first step in procathepsin D processing, which depends on transport of the proenzyme from the TGN to the late

endosomes (Rijnboutt et al., 1992; Delbruck et al., 1994). Previous reports have indicated that hVps34 is localized predominantly in Golgi membranes (Kihara et al., 2001a) and that inhibition of PI 3-kinase activity with wortmannin causes intracellular accumulation of unprocessed procathepsin D, which then enters the secretory pathway (Davidson, 1995). Follow-up studies by Row et al. implicated Vps34 as the probable wortmannin target by showing that overexpression of a kinase-deficient form of rat Vps34 produced a similar impairment in procathepsin D conversion to the 47-48 kDa endosomal intermediate (Row et al., 2001). The discrepancy between these earlier results and the present findings based on siRNA-mediated silencing of hVps34 could be related to differences in the mechanisms used for interference with hVps34 function. For instance, siRNA is expected to eliminate endogenous hVps34 and deplete PtdIns(3)*P* at specific subcellular sites where the enzyme normally catalyzes the production of this phospholipid. By contrast, overexpression of a kinase-deficient form of Vps34 might act by competing with endogenous hVps34 for binding to the p150 adaptor (Panaretou et al., 1997) or other interacting proteins such as Rab5 (Murray et al., 2002) and Rab7 (Stein et al., 2003). This might cause perturbations of protein trafficking pathways as a result of titration of Vps34 partners, but not necessarily due to loss of PtdIns(3)*P* production by endogenous hVps34.

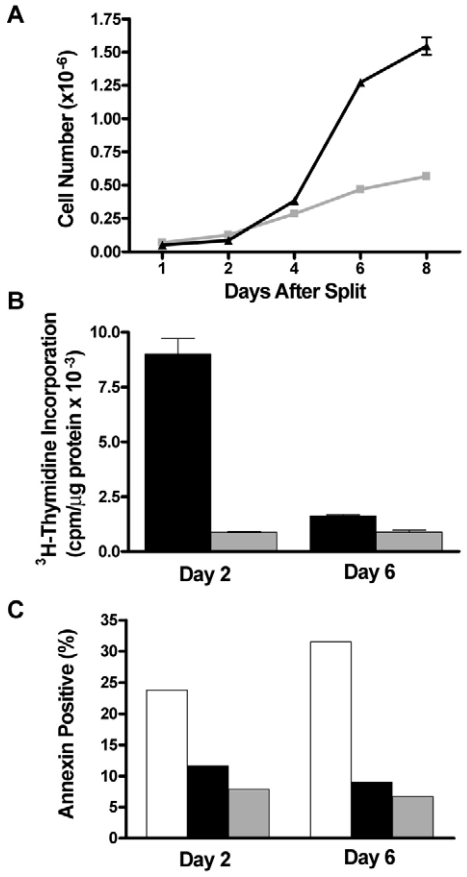

Fig. 12. hVps34 KD cells exhibit a marked reduction in growth rate. (A) Following 2 days of selection, control (black) and hVps34 KD (gray) cells were seeded in 35 mm dishes at an equal density of 50,000 cells/dish. At the indicated time points, triplicate dishes from each cell line were harvested and counted with a Coulter Z1 particle counter (mean±s.e.m.). (B) Control (black) and KD (gray) cells were seeded in 25 cm^2 flasks at 150,000 cells/flask. On the indicated days, triplicate flasks of each cell line were incubated with [^{3}H]thymidine (1.0 μCi/ml) for 5 hours. Radioactivity incorporated into TCA-precipitable material was counted and normalized to total cellular protein (mean±s.e.m.). (C) Control (black) and KD (gray) cells were seeded in 60 mm dishes at 200,000 cells/dish. On the indicated days, duplicate dishes from each cell line were harvested and stained with annexin-V. Annexin-positive cells were counted using a Guava personal cytometer. Cells treated overnight with TNF-α (white) served as a positive control for apoptosis.

If hVps34 is not specifically responsible for producing PtdIns(3)*P* needed for vesicular trafficking of cathepsin D out of the TGN, it is conceivable that other closely related PI 3-kinases might fulfill this role. In this regard, it is worth mentioning two novel PI 3-kinase activities that could serve as potential alternate sources of PtdIns(3)*P* in the Golgi compartment. Both appear to be required for genesis of constitutive transport vesicles in the TGN. The first is associated with TGN38 and a regulatory complex termed p62^{cplx} (Jones et al., 1998). The second was found to associate with TGN46 (Hickinson et al., 1997). Neither of these PI 3-kinases has yet been characterized in sufficient detail to indicate how closely they might be related to Vps34 or if they might be required for endosome- and lysosome-directed trafficking of proenzymes associated with the M6PR.

Our finding that hVps34 knockdown had little or no effect on EEA1 localization or early endocytic trafficking, yet severely affected late endosome morphology and function, was quite unexpected. Previous studies using FYVE-domain probes have demonstrated that PtdIns(3)*P* is concentrated in microdomains in the membranes surrounding early endosomes, as well as in the internal vesicles of MVEs (Gillooly et al., 2003; Gillooly et al., 2000). Therefore, the most obvious implication of our findings is that knockdown of hVps34 results in a more extreme depletion of PtdIns(3)*P* in the late endosomes than in the early endosomes. We did not attempt to perform direct phospholipid analyses on early and late endosome fractions because of the difficulty of accumulating large numbers of hVps34 KD cells. However, our studies with the GFP-2xFYVE probe support the notion that PtdIns(3)*P* depletion is more severe in LAMP1-positive compartments than in LAMP1-negative vesicles (Fig. 7). One possible explanation for this observation is that the small amount of residual hVps34 remaining in the KD cells is selectively directed to early endosomes where it can preserve the PtdIns(3)*P* pool. Although we cannot rule this out, we believe that a more likely possibility is that early endosomes have alternative pathways for producing PtdIns(3)*P*, whereas late endosomes are more dependent on hVps34.

One alternative pathway that could produce sufficient PtdIns(3)*P* to maintain early endosome function might include a type I PI 3-kinase, working in tandem with phosphoinositide 4- and 5-phosphatases. Type I PI 3-kinases are heterodimers composed of p110 catalytic subunits and p85 or p55 regulatory subunits (Vanhaesebroeck et al., 2001). The large increase in cellular phosphatidylinositol (3,4,5)-trisphosphate [PtdIns(3,4,5)P_3] typically observed upon stimulation of type I enzymes suggests that phosphatidylinositol (4,5)-bisphosphate [PtdIns(4,5)P_2] is the preferred substrate in vivo (Fruman et al.,

1998; Leevers et al., 1999). The potential exists for PtdIns(3)*P* to be generated from PtdIns(3,4,5)P_3 through the sequential actions of inositol-polyphosphate 5-phosphatase (Kisseleva et al., 2000) and inositol-polyphosphate 4-phosphatase (Norris et al., 1995; Norris et al., 1997), which are capable of removing the 5′-phosphate and the 4′-phosphate from PtdIns(3,4,5)P_3 and PtdIns(3,4)P_2, respectively. Indeed, in a recent study utilizing function-blocking antibodies, Shin et al. demonstrated that a Rab5-regulated enzyme cascade consisting of PI 3-kinase β (p110β-p85α) and two phosphatases (PI 5- and PI 4-phosphatases) might generate as much as 30% of the PtdIns(3)*P* in early endosomal fractions (Shin et al., 2005). Furthermore, by silencing the expression of the PI 4-phosphatase, they demonstrated that this pathway is functionally important for endocytosis and maintenance of PtdIns(3)*P* levels in Hela cells. Finally, in astrocytes from *weeble* mice that carry a loss-of-function mutation in the gene for the PI 4-phosphatase, intracellular PtdIns(3)*P* levels were reduced by 27% compared with wild-type cells. The studies with *weeble* mice raise the intriguing possibility that a similar type I PI 3-kinase β kinase and/or phosphatase enzyme cascade could contribute to maintaining the pool of PtdIns(3)*P* needed for EEA1 localization and vesicular trafficking in the early endosome compartment of tumor cells of astrocytic origin. Such an alternative pathway could be particularly important in tumors where PTEN mutations frequently occur. For example, in the absence of an active PTEN phosphoinositide 3-phosphatase, the pool of PtdIns(3,4,5)P_3 available to generate PtdIns(3)*P* through the PI 4-phosphatase and PI 5-phosphatase cascade could be substantially increased.

Another alternative mechanism to generate PtdIns(3)*P* could involve a type II PI 3-kinase (e.g. PI 3-kinase C2α). The type II PI 3-kinases remain poorly understood, but there is some evidence that they are localized in the TGN and clathrin-coated vesicles (Prior and Clague, 1999). Indeed, it is quite likely that type II PI 3-kinase can produce PtdIns(3)*P* in mammalian cells, since these enzymes preferentially phosphorylate phosphatidylinositol over PtdIns(4)*P* and PtdIns(4,5)P_3 in vitro (Arcaro et al., 1998; Fruman et al., 1998). The type II PI 3-kinases are less sensitive to wortmannin than hVps34 and type I PI 3-kinases. Thus, our observation that EEA1 localization is sensitive to 1 μM wortmannin but not 0.1 μM wortmannin (Fig. 6) is consistent with the possibility that a type II PI 3-kinase contributes to maintaining the PtdIns(3)*P* pool in early endosomes in the hVps34 KD cells. Ultimately, siRNA knockdown studies of individual type I and type II PI 3-kinases and associated phosphatases may have to be combined with the knockdown of hVps34 to dissect the specific alternative source of PtdIns(3)*P* in the early endosome compartment of mammalian cells. These studies are likely to be quite challenging, in light of the apparent requirement for a minimal level of PtdIns(3)*P* to maintain cell growth (discussed below).

There have been conflicting reports regarding the importance of PI 3-kinase for post-endocytic sorting of activated receptors that enter the cell through clathrin-coated pits. In one study, wortmannin inhibited the formation of internal vesicles in the MVE compartments of HEp2 cells, but the EGFR was still able to reach the perimeter membrane of lysosomes, exposing the N-terminal ligand-binding domain to a degradative environment (Futter et al., 2001). However, in another study with BHK-21 cells (Petiot et al., 2003), wortmannin treatment prevented the translocation of ligand-stimulated EGFR from early endosomes to late endosomes. Our results (Fig. 9A) support the conclusion that hVps34 is not absolutely essential for translocation of activated EGFR to late endosomes in U-251 cells. Degradation of EGFR ultimately occurs in the absence of hVps34 (Fig. 9B), apparently because the enlarged vacuoles retain the capacity for fusion with pre-existing lysosomes. However, the failure of inward vesiculation appears to slow the initial rate of EGFR delivery to lysosomes. Interestingly, prior to degradation, a much higher proportion of the EGFR pool in the hVps34 KD cells remains in a phosphorylated state capable of activating the ERK pathway (Fig. 10). One mechanism for dephosphorylation of EGFR involves protein tyrosine phosphatase 1B on the surface of the endoplasmic reticulum (Haj et al., 2002). However, the possibility that tyrosine dephosphorylation might occur in conjunction with internalization of the EGFR into the MVEs has also been suggested (Gill, 2002). Since the phosphorylated C-terminal domain of the EGFR on the surface of endosomes is capable of interacting with cytoplasmic adaptors and signaling to the ERK pathway (Burke et al., 2001; Wiley and Burke, 2001), we conclude that, in the absence of PtdIns(3)*P* generated by hVps34, an increased proportion of the EGFR is retained on the surface of the enlarged endosomes in an active phosphorylated state prior to eventual degradation of the N-terminal domain by lysosomal proteases.

The morphological phenotype of the hVps34 KD cells resembles the ‘class E’ vacuolar phenotype that can be triggered in mammalian cells by interfering with the assembly of the ESCRT-III complex on MVEs (Babst et al., 1998; Bishop and Woodman, 2000). This suggests a molecular mechanism whereby suppression of hVps34 might cause a failure of inward vesiculation of MVEs. Specifically, PtdIns(3,5)P_2 has been identified as an important phospholipid for membrane recruitment of hVps24, a key component of ESCRT-III (Whitley et al., 2003). Since the kinase responsible for generating PtdIns(3,5)P_3 is in fact a PtdIns(3)*P*-binding FYVE-domain protein termed PIKfyve (Sbrissa et al., 1999; Ikonomov et al., 2003), reduced expression of hVps34 and localized depletion of PtdIns(3)*P* might prevent membrane recruitment of PIKfyve and the subsequent PtdIns(3,5)P_3-dependent assembly of ESCRT-III. Further investigation of this possibility will have to await the development of antibodies that can reliably detect endogenous PIKfyve by immunofluorescence.

In addition to the striking morphological changes affecting the late endosome compartment, we noted a markedly reduced growth rate in the hVps34 KD cells (Fig. 12). This observation is consistent with studies in *Caenorhabditis elegans*, where loss-of-function mutations in the gene encoding the hVps34 ortholog LET-512/Vps34 are associated with an embryonic lethal phenotype (Roggo et al., 2002). A recent report has implicated Vps34 in the nutrient-sensitive regulation of p70 S6-kinase (Byfield et al., 2005). Thus, disruption of the regulation of translation could be one mechanism underlying the growth inhibitory effects of Vps34 knockdown. In an earlier study, Siddhanta et al. found that a neutralizing antibody against hVps34 could block the insulin-stimulated increase in DNA synthesis in GRC-LR+73 cells only when it was microinjected during a defined temporal window of the G1 phase of the cell cycle (Siddhanta et al., 1998). This raises the

intriguing possibility that, in addition to its roles in membrane sorting in MVEs and the regulation of p70 S6-kinase, hVps34 might play a specific role in the control of DNA replication and/or transcription. Although this possibility remains to be explored in mammalian cells, studies using plant cells have found that Vps34 is associated with discrete nuclear and nucleolar transcription sites (Drobak et al., 1995; Bunney et al., 2000). In light of these observations, the prospect of a role for hVp34 in the nucleus of mammalian cells promises to be an important topic for future study.

Materials and Methods

hVps34 gene silencing

U-251 human glioblastoma cells were obtained from the DCT Tumor Repository (National Cancer Institute) and were maintained in Dulbecco's modified Eagle medium (DMEM), supplemented with 10% fetal bovine serum (FBS). The pSUPER.retro.puro vector was obtained from OligoEngine. Two short hairpin RNAs were designed to target 19 bp sequences specific to human Vps34 mRNA. The oligonucleotide sequences used for siRNA interference with hVps34 expression corresponded to $5'\text{-}_{675}$GTGTGATGATAAGGAATAT$_{693}$-$3'$ (KD) and $5'\text{-}_{135}$GTTCTCAGGACTATATCAA$_{153}$-$3'$ (KD2) of the human *VPS34* cDNA sequence (GenBank: BC033004), followed by a 9-nucleotide non-complimentary spacer (TTCAAGAGA) and the reverse compliment of the initial 19-nucleotide sequence. The control siRNA target sequence, $5'\text{-}_{395}$AATACGGCATGTCTCGCCA$_{413}$-$3'$, contained a single base mismatch (underlined) at position 407 from the *hVPS34* sequence and it did not match any other known sequences in the GenBank database. Retrovirus was produced in HEK293 GPG packaging cells (Ory et al., 1996) maintained in DMEM + 10% heat-inactivated FBS with 1 μg/ml puromycin, 300 μg/ml G418 and 2 μg/ml doxycycline. For transfection, the HEK293 GPG cells were seeded at 1.2×10^7 cells/dish on 100 mm dishes in DMEM containing 10% heat-inactivated FBS. 24 hours later, the cells were transfected with pSUPER.retro.puro constructs using Lipofectamine-Plus reagent (Invitrogen). 48 and 72 hours after transfection, the virus-enriched medium was collected and passed through a 0.22 μm filter. Infections of the U-251 cells were performed on three sequential days in the presence of 4.0 μg/ml hexadimethrine bromide (Sigma). Cells were then trypsinized and re-plated in selection medium containing 1 μg/ml puromycin.

For each experiment, control and hVps34-knockdown (KD) cell lines were harvested in order to verify the decrease in hVps34 expression. Briefly, equal amounts of protein were subjected to SDS-PAGE and immunoblot analysis using a polyclonal antibody against hVps34 (Zymed Laboratories), followed by horseradish peroxidase (HRP)-conjugated goat anti-rabbit IgG and enhanced chemiluminescent (ECL) detection reagent (Amersham-Pharmacia Biotech) (Wilson et al., 1996). Antibodies against unrelated proteins such as lamin B_2 (Zymed Laboratories), lactate dehydrogenase (LDH) (Sigma) and calreticulin (Stressgen) were used to check for nonspecific effects of the siRNA. Immunoblot signals were quantified using a Kodak 440CF Image Station.

Characterization of vacuoles by immunofluorescence microscopy

Phase contrast images of control and hVps34 KD cells were obtained using an Olympus IX70 inverted microscope equipped with a digital camera, using SPOT imaging software (Diagnostic Instruments). For immunofluorescence studies, cells were seeded on laminin-coated glass coverslips in 35 mm dishes at 100,000 cells per dish. 24 hours later, cells were washed with PBS, fixed with ice-cold methanol for 10 minutes, and blocked with 10% goat serum in PBS for 30 minutes. The following primary antibodies were applied for 1 hour in PBS with 10% goat serum: anti-LAMP1 (University of Iowa Developmental Studies Hybridoma Bank), anti-LGP85 (gift from Y. Tanaka, Kyushu University, Fukuoka, Japan), anti-M6PR and anti-calreticulin (Affinity Bioreagents), anti-GM130 (BD Biosciences), and anti-LBPA (gift from T. Kobayashi, RIKEN Frontier Research System, Saitama, Japan). Cells were washed three times with 10% goat serum in PBS, then incubated for 1 hour with Alexa Fluor 568 goat anti-mouse (1:800; Molecular Probes) or Alexa Fluor 488 goat anti-rabbit IgG (1:500; Molecular Probes) in PBS with 10% goat serum. After washing three times with PBS, the coverslips containing the cells were mounted with DAKO fluorescent mounting medium and photomicrographs were taken with a Nikon Eclipse 800 fluorescence microscope equipped with a Sensys digital camera and ImagePro software (Media Cybernetics).

To visualize acidic intracellular compartments, cells were incubated with Acridine Orange (2.5 μg/ml; Molecular Probes) in serum-free, Phenol Red-free DMEM for 30 minutes at 37°C. Cells were then washed twice and the coverslips were immediately inverted onto a drop of serum-free DMEM containing 20% glycerol and examined by fluorescence microscopy.

To highlight the endosomal and lysosomal compartments, cells were incubated with a fluid-phase tracer, Texas Red-dextran (10,000 M_r, 500 μg/ml; Molecular Probes) in Phenol Red-free DMEM with 10% FBS for 16 hours at 37°C. Following incubation for 2 hours in dextran-free DMEM, cells were washed with PBS, fixed with ice-cold methanol, and stained with anti-LAMP1 followed by FITC-conjugated goat anti-mouse IgG (Sigma).

Electron microscopy

For transmission electron microscopy (EM), cell pellets fixed with 3% glutaraldehyde for 1 hour were washed three times for 10 minutes with 0.2 M sodium cacodylate, post-fixed for 2 hours with 1% OsO_4 followed by 1 hour with saturated uranyl acetate. Dehydration was carried out by a graded series of chilled ethanol solutions (30-100%) and a final dehydration with 100% acetone. Cells were infiltrated overnight in Spurr's resin (Electron Microscope Sciences) and ultrathin sections were obtained and collected on copper 300-mesh support grids. Sections were stained with uranyl acetate and lead citrate, and examined using a Philips CM 10 transmission electron microscope.

For immunogold staining of cathepsin D, cell pellets were fixed with 1% glutaraldehyde and washed sequentially with cacodylate buffer and 50 mM ammonium chloride. Following dehydration with ethanol only, the cells were infiltrated and embedded in LR White® embedding media (London Resin). Sections were collected with gold support grids and blocked with a solution of 10% fish gelatin in PBS for 1 hour and incubated for 2 hours with goat anti-cathepsin D antibody (Santa Cruz Biotechnology) (1:40 dilution in PBS) followed by 1 hour with donkey anti-goat IgG conjugated with 6 nm colloidal gold (Jackson ImmunoResearch Labs). The samples were post-fixed with 1% glutaraldehyde, washed, and stained with uranyl acetate and lead citrate.

Metabolic labeling and immunoprecipitation of cathepsin D

Cells were seeded in 100 mm dishes at 350,000 cells per dish in medium containing 1 μg/ml puromycin. After 24 hours, the cells were washed and incubated for 30 minutes in methionine-free DMEM containing 10% FBS. The cultures were labeled for 30 minutes in the same medium containing 100 μCi/ml [^{35}S]methionine/cysteine (Easy Tag™ EXPRESS, 1.18 μCi/mmol; NEN/PerkinElmer), washed once with PBS, and then chased in complete medium supplemented with 200 μM methionine and 200 μM cysteine for 4 hours. At the end of the chase, cells were washed twice, scraped into ice-cold PBS, and collected by centrifugation for 5 minutes at 400 ***g***. Cell lysates were prepared in 200 μl RIPA buffer (100 mM Tris-HCl, pH 7.4, 2 mM EDTA, 0.5% Nonidet P-40, 0.1% SDS, 0.5% sodium deoxycholate) supplemented with complete mini protease inhibitors (Roche). Insoluble material was removed by centrifugation at 100,000 ***g*** for 1 hour at 4°C and the soluble fractions were pre-cleared by incubation with protein A sepharose beads for 30 minutes at 4°C. After removal of the beads, immunoprecipitation was performed essentially as previously described (Dugan et al., 1995), using a polyclonal antibody against cathepsin D (Biodesign International). SDS-PAGE and fluorographic analysis of the immunoprecipitated proteins was performed by standard methods (Wilson et al., 1998). Immunoblotting for total cellular cathepsin D was performed as described earlier, using a goat polyclonal antibody against cathepsin D (Santa Cruz Biotechnology).

Endocytosis of HRP

Cells were washed with DMEM and incubated with 2 mg/ml HRP (Sigma) in DMEM containing 1% BSA at 37°C. At designated time points, cells were placed on ice, washed three times with ice-cold PBS containing 1% BSA and one time with PBS alone. Cells were scraped from the dish into PBS, pelleted by centrifugation, washed once more with PBS and then disrupted in PBS containing 0.5% Triton X-100. Cell lysates were clarified by centrifugation at 10,000 ***g*** for 5 minutes at 4°C, and HRP activity in the supernatant was determined using a Turbo TMB enzyme-linked immunosorbent assay kit (Pierce Chemical). Results were normalized to protein, measured with a BCA protein assay kit (Pierce Chemical).

Transferrin receptor recycling

Cells were pre-incubated in serum-free DMEM for 1 hour, then incubated for 30 minutes at 37°C with 50 μg/ml biotinylated holo-transferrin (Sigma) in serum-free medium. The cultures were placed on ice, washed twice with ice-cold DMEM, and then stripped in 10 mM acetic acid, 150 mM NaCl (pH 3.5) for 1 minute to remove residual surface-bound transferrin. Cells were chased for the indicated time periods in medium containing 0.5 mg/ml unlabeled holo-transferrin and 0.1 mM deferoxamine mesylate. At each time point, the medium was collected and the cells were lysed in 50 mM HEPES, pH 7.4, 150 mM NaCl, 10 mM EDTA, 2 mM EGTA, 1% Triton X-100 and 0.1% SDS. Samples of medium and cell lysate were mixed with 5× concentrated SDS sample buffer and subjected to SDS-PAGE. Proteins were transferred to polyvinylidene fluoride (PVDF) membranes and the biotinylated transferrin was detected by ECL following incubation with streptavidin-HRP. ECL signals were quantified with the Kodak 440 CF Image Station.

EGFR internalization and degradation

Cells infected with the hVps34 KD or control vectors were selected for 5 days and seeded at equal density in 60 mm dishes. On the following day, the cells were switched to serum-free medium and maintained for 16 hours to allow the EGFR to

accumulate on the cell surface. Receptor internalization and degradation were then stimulated by addition of EGF (100 ng/ml; Upstate Biotechnology). At designated intervals after addition of EGF, cells were washed twice with ice-cold PBS and harvested in SDS-PAGE sample buffer. Equal amounts of protein were then subjected to SDS-PAGE and immunoblot analysis, using antibodies against total EGFR (BD Biosciences), phospho-EGFR (Cell Signaling Technology), phospho-ERK and total ERK (Cell Signaling Technology). ECL signals were quantified directly with the Kodak Image Station, as described above, or by densitometry after film exposure. In a separate study, cells were fixed in methanol at intervals after EGF stimulation, and localization of the receptor was determined by immunofluorescence analysis as described earlier, using the antibody against total EGFR.

Subcellular distribution of EEA1

Cells were trypsinized and collected by centrifugation at 400 ***g*** for 5 minutes at 4°C. Cell pellets were washed three times with ice-cold PBS and allowed to swell for 15 minutes at 4°C in hypotonic buffer (10 mM HEPES, pH 7.5, 1.5 mM $MgCl_2$, 10 mM KCl, 1 mM DTT and protease inhibitors). The cells were disrupted with 15 strokes of a Teflon homogenizer and sucrose was added to a final concentration of 0.25 M. Soluble and particulate fractions were obtained by centrifugation at 100,000 ***g*** for 1 hour at 4°C. Equal percentages of the soluble and particulate fractions were subjected to SDS-PAGE and immunoblot analysis using an antibody against EEA1 (BD Biosciences). ECL signals were quantified by densitometry, using the Kodak 440CF Image Station. For immunofluorescent localization of EEA1, cells were fixed with 3% paraformaldehyde for 15 minutes at room temperature, quenched with 50 mM NH_4Cl in PBS (5 minutes), permeabilized with 50 μg/ml digitonin in PBS (5 minutes), and blocked with 10% goat serum in PBS for 30 minutes. Anti-EEA1 was then applied for 1 hour followed by Alexa Fluor 568 goat anti-mouse IgG.

Localization of PtdIns(3)*P* with a GFP-FYVE probe

After 4 days of selection, cells infected with the hVps34 knockdown and control vectors were seeded on laminin-coated glass coverslips in 35 mm dishes at 100,000 cells per dish. 24 hours later, cells were transfected with pEGFP-2xFYVE (Petiot et al., 2003) (provided by H. Stenmark, Norwegian Radium Hospital, Oslo, Norway) using Lipofectamine-Plus reagent. 16 hours later, the coverslips were fixed in methanol and processed for immunofluorescence as described earlier, using Living Colors® anti-GFP (BD Biosciences) to detect the GFP-2xFYVE probe, and anti-LAMP1 antibody to detect late endosome and lysosome compartments.

Cell growth and survival

To assess cell growth, hVps34 KD or control cells that had been selected for two days were seeded in 35 mm dishes at 50,000 cells per dish. On specified days, the cells were trypsinized and counted using a Coulter Z-series particle counter (Beckman-Coulter Corporation). To measure DNA synthesis, cells were seeded in 25 cm^2 flasks at 150,000 cells per flask. On days 2 and 6, cells were incubated for 5 hours in medium containing 1 μCi/ml [methyl-^{3}H]thymidine (5 Ci/mmol; Amersham Biosciences). Incorporation of radioactivity into TCA-precipitable material was determined as described previously (Maltese et al., 1981).

For assessment of apoptotic cell death, cells were seeded in 60 mm dishes at 200,000 cells per dish. On days 2 and 6, floating and adherent cells were harvested and stained with annexin-V and 7-amino-actinomycin D as described in the protocol for the Guava Nexin™ kit (Guava Technologies). Staining was quantified using a Guava personal cytometer. Control cells treated for 18 hours with 10 ng/ml TNF-α (Calbiochem) plus 2.5 μg/ml cyclohexamide (Sigma) served as a positive control for apoptosis.

This work was supported in part by grants from the NIH (RO1CA34569) and the U.S. DOD (Idea Award W81XWH-04-1-0493).

References

Arcaro, A., Volinia, S., Zvelebil, M. J., Stein, R., Watton, S. J., Layton, M. J., Gout, I., Ahmadi, K., Downward, J. and Waterfield, M. D. (1998). Human phosphoinositide 3-kinase C2beta, the role of calcium and the C2 domain in enzyme activity. *J. Biol. Chem.* **273**, 33082-33090.

Babst, M., Wendland, B., Estepa, E. J. and Emr, S. D. (1998). The Vps4p AAA ATPase regulates membrane association of a Vps protein complex required for normal endosome function. *EMBO J.* **17**, 2982-2993.

Bishop, N. and Woodman, P. (2000). ATPase-defective mammalian VPS4 localizes to aberrant endosomes and impairs cholesterol trafficking. *Mol. Biol. Cell* **11**, 227-239.

Brown, W. J., DeWald, D. B., Emr, S. D., Plutner, H. and Balch, W. E. (1995). Role for phosphatidylinositol 3-kinase in the sorting and transport of newly synthesized lysosomal enzymes in mammalian cells. *J. Cell Biol.* **130**, 781-796.

Brummelkamp, T. R., Bernards, R. and Agami, R. (2002). A system for stable expression of short interfering RNAs in mammalian cells. *Science* **296**, 550-553.

Bucci, C., Thomsen, P., Nicoziani, P., McCarthy, J. and van Deurs, B. (2000). Rab7: a key to lysosome biogenesis. *Mol. Biol. Cell* **11**, 467-480.

Bunney, T. D., Watkins, P. A., Beven, A. F., Shaw, P. J., Hernandez, L. E., Lomonossoff, G. P., Shanks, M., Peart, J. and Drobak, B. K. (2000). Association of phosphatidylinositol 3-kinase with nuclear transcription sites in higher plants. *Plant Cell* **12**, 1679-1688.

Burke, P., Schooler, K. and Wiley, H. S. (2001). Regulation of epidermal growth factor receptor signaling by endocytosis and intracellular trafficking. *Mol. Biol. Cell* **12**, 1897-1910.

Byfield, M. P., Murray, J. T. and Backer, J. M. (2005). hVps34 is a nutrient-regulated lipid kinase required for activation of p70 S6 kinase. *J. Biol. Chem.* **280**, 33076-33082.

Cheever, M. L., Sato, T. K., de Beer, T., Kutateladze, T. G., Emr, S. D. and Overduin, M. (2001). Phox domain interaction with PtdIns(3)P targets the Vam7 t-SNARE to vacuole membranes. *Nat. Cell Biol.* **3**, 613-618.

Christoforidis, S., McBride, H. M., Burgoyne, R. D. and Zerial, M. (1999). The Rab5 effector EEA1 is a core component of endosome docking. *Nature* **397**, 621-625.

Cormont, M., Mari, M., Galmiche, A., Hofman, P. and Marchand-Brustel, Y. (2001). A FYVE-finger-containing protein, Rabip4, is a Rab4 effector involved in early endosomal traffic. *Proc. Natl. Acad. Sci. USA* **98**, 1637-1642.

Corvera, S. (2001). Phosphatidylinositol 3-kinase and the control of endosome dynamics: new players defined by structural motifs. *Traffic* **2**, 859-866.

Corvera, S., D'Arrigo, A. and Stenmark, H. (1999). Phosphoinositides in membrane traffic. *Curr. Opin. Cell Biol.* **11**, 460-465.

Davidson, H. W. (1995). Wortmannin causes mistargeting of procathepsin D. evidence for the involvement of a phosphatidylinositol 3-kinase in vesicular transport to lysosomes. *J. Cell Biol.* **130**, 797-805.

Delbruck, R., Desel, C., von Figura, K. and Hille-Rehfeld, A. (1994). Proteolytic processing of cathepsin D in prelysosomal organelles. *Eur. J. Cell Biol.* **64**, 7-14.

Drobak, B. K., Watkins, P. A., Bunney, T. D., Dove, S. K., Shaw, P. J., White, I. R. and Millner, P. A. (1995). Association of multiple GTP-binding proteins with the plant cytoskeleton and nuclear matrix. *Biochem. Biophys. Res. Commun.* **210**, 7-13.

Dugan, J. M., deWit, C., McConlogue, L. and Maltese, W. A. (1995). The ras-related GTP binding protein, Rab1B, regulates early steps in exocytic transport and processing of β-amyloid precursor protein. *J. Biol. Chem.* **270**, 10982-10989.

Fruman, D. A., Meyers, R. E. and Cantley, L. C. (1998). Phosphoinositide kinases. *Annu. Rev. Biochem.* **67**, 481-507.

Fruman, D. A., Rameh, L. E. and Cantley, L. C. (1999). Phosphoinositide binding domains: embracing 3-phosphate. *Cell* **97**, 817-820.

Futter, C. E., Collinson, L. M., Backer, J. M. and Hopkins, C. R. (2001). Human VPS34 is required for internal vesicle formation within multivesicular endosomes. *J. Cell Biol.* **155**, 1251-1264.

Ghosh, P., Dahms, N. M. and Kornfeld, S. (2003). Mannose 6-phosphate receptors: new twists in the tale. *Nat. Rev. Mol. Cell. Biol.* **4**, 202-212.

Gill, G. N. (2002). A pit stop at the ER. *Science* **295**, 1654-1655.

Gillooly, D. J., Morrow, I. C., Lindsay, M., Gould, R., Bryant, N. J., Gaullier, J. M., Parton, R. G. and Stenmark, H. (2000). Localization of phosphatidylinositol 3-phosphate in yeast and mammalian cells. *EMBO J.* **19**, 4577-4588.

Gillooly, D. J., Raiborg, C. and Stenmark, H. (2003). Phosphatidylinositol 3-phosphate is found in microdomains of early endosomes. *Histochem. Cell Biol.* **120**, 445-453.

Gough, N. R., Zweifel, M. E., Martinez-Augustin, O., Aguilar, R. C., Bonifacino, J. S. and Fambrough, D. M. (1999). Utilization of the indirect lysosome targeting pathway by lysosome-associated membrane proteins (LAMPs) is influenced largely by the C-terminal residue of their GYXXphi targeting signals. *J. Cell Sci.* **112**, 4257-4269.

Gruenberg, J. and Maxfield, F. R. (1995). Membrane transport in the endocytic pathway. *Curr. Opin. Cell Biol.* **7**, 552-563.

Haj, F. G., Verveer, P. J., Squire, A., Neel, B. G. and Bastiaens, P. I. H. (2002). Imaging sites of receptor dephosphorylation by PTP1B on the surface of the endoplasmic reticulum. *Science* **295**, 1708-1711.

Hentze, M., Hasilik, A. and von Figura, K. (1984). Enhanced degradation of cathepsin D synthesized in the presence of the threonine analog beta-hydroxynorvaline. *Arch. Biochem. Biophys.* **230**, 375-382.

Herman, P. K., Stack, J. H. and Emr, S. D. (1992). An essential role for a protein and lipid kinase complex in secretory protein sorting. *Trends Cell Biol.* **2**, 363-368.

Hickinson, D. M., Lucocq, J. M., Towler, M. C., Clough, S., James, J., James, S. R., Downes, C. P. and Ponnambalam, S. (1997). Association of a phosphatidylinositol-specific 3-kinase with a human trans-Golgi network resident protein. *Curr. Biol.* **7**, 987-990.

Hirst, J., Futter, C. E. and Hopkins, C. R. (1998). The kinetics of mannose 6-phosphate receptor trafficking in the endocytic pathway in HEp-2 cells: the receptor enters and rapidly leaves multivesicular endosomes without accumulating in a prelysosomal compartment. *Mol. Biol. Cell* **9**, 809-816.

Ikonomov, O. C., Sbrissa, D., Foti, M., Carpentier, J. L. and Shisheva, A. (2003). PIKfyve controls fluid phase endocytosis but not recycling/degradation of endocytosed receptors or sorting of procathepsin D by regulating multivesicular body morphogenesis. *Mol. Biol. Cell* **14**, 4581-4591.

Jones, S. M., Alb, J. G., Jr, Phillips, S. E., Bankaitis, V. A. and Howell, K. E. (1998). A phosphatidylinositol 3-kinase and phosphatidylinositol transfer protein act synergistically in formation of constitutive transport vesicles from the trans-Golgi network. *J. Biol. Chem.* **273**, 10349-10354.

Kanai, F., Liu, H., Field, S. J., Akbary, H., Matsuo, T., Brown, G. E., Cantley, L. C. and Yaffe, M. B. (2001). The PX domains of p47phox and p40phox bind to lipid products of PI(3)K. *Nat. Cell Biol.* **3**, 675-678.

Kanzawa, T., Kondo, Y., Ito, H., Kondo, S. and Germano, I. (2003). Induction of autophagic cell death in malignant glioma cells by arsenic trioxide. *Cancer Res.* **63**, 2103-2108.

Katzmann, D. J., Odorizzi, G. and Emr, S. D. (2002). Receptor downregulation and multivesicular-body sorting. *Nat. Rev. Mol. Cell. Biol.* **3**, 893-905.

Kauppi, M., Simonsen, A., Bremnes, B., Vieira, A., Callaghan, J., Stenmark, H. and Olkkonen, V. M. (2002). The small GTPase Rab22 interacts with EEA1 and controls endosomal membrane trafficking. *J. Cell Sci.* **115**, 899-911.

Kihara, A., Kabeya, Y., Ohsumi, Y. and Yoshimori, T. (2001a). Beclin-phosphatidylinositol 3-kinase complex functions at the trans- Golgi network. *EMBO Rep.* **2**, 330-335.

Kihara, A., Noda, T., Ishihara, N. and Ohsumi, Y. (2001b). Two distinct Vps34 phosphatidylinositol 3-kinase complexes function in autophagy and carboxypeptidase Y sorting in Saccharomyces cerevisiae. *J. Cell Biol.* **152**, 519-530.

Kisseleva, M. V., Wilson, M. P. and Majerus, P. W. (2000). The isolation and characterization of a cDNA encoding phospholipid-specific inositol polyphosphate 5-phosphatase. *J. Biol. Chem.* **275**, 20110-20116.

Kobayashi, T., Stang, E., Fang, K. S., de Moerloose, P., Parton, R. G. and Gruenberg, J. (1998). A lipid associated with the antiphospholipid syndrome regulates endosome structure and function. *Nature* **392**, 193-197.

Kuronita, T., Eskelinen, E. L., Fujita, H., Saftig, P., Himeno, M. and Tanaka, Y. (2002). A role for the lysosomal membrane protein LGP85 in the biogenesis and maintenance of endosomal and lysosomal morphology. *J. Cell Sci.* **115**, 4117-4131.

Le Borgne, R. and Hoflack, B. (1998). Protein transport from the secretory to the endocytic pathway in mammalian cells. *Biochim. Biophys. Acta* **1404**, 195-209.

Leevers, S. J., Vanhaesebroeck, B. and Waterfield, M. D. (1999). Signalling through phosphoinositide 3-kinases: the lipids take centre stage. *Curr. Opin. Cell Biol.* **11**, 219-225.

Li, G. and Stahl, P. D. (1993). Structure-function relationship of the small GTPase rab5. *J. Biol. Chem.* **268**, 24475-24480.

Maltese, W. A., Reitz, B. A. and Volpe, J. J. (1981). Effects of isoleucine deprivation on synthesis of sterols and fatty acids in LM-cells. *J. Biol. Chem.* **256**, 2185-2193.

Mayran, N., Parton, R. G. and Gruenberg, J. (2003). Annexin II regulates multivesicular endosome biogenesis in the degradation pathway of animal cells. *EMBO J.* **22**, 3242-3253.

Meyers, R. and Cantley, L. C. (1997). Cloning and characterization of a wortmannin-sensitive human phosphatidylinositol 4-kinase. *J. Biol. Chem.* **272**, 4384-4390.

Murray, J. T., Panaretou, C., Stenmark, H., Miaczynska, M. and Backer, J. M. (2002). Role of Rab5 in the recruitment of hVps34/p150 to the early endosome. *Traffic* **3**, 416-427.

Nielsen, E., Christoforidis, S., Uttenweiler-Joseph, S., Miaczynska, M., Dewitte, F., Wilm, M., Hoflack, B. and Zerial, M. (2000). Rabenosyn-5, a novel Rab5 effector, is complexed with hVPS45 and recruited to endosomes through a FYVE finger domain. *J. Cell Biol.* **151**, 601-612.

Nissler, K., Strubel, W., Kreusch, S., Rommerskirch, W., Weber, E. and Wiederanders, B. (1999). The half-life of human procathepsin S. *Eur. J. Biochem.* **263**, 717-725.

Norris, F. A., Auethavekiat, V. and Majerus, P. W. (1995). The isolation and characterization of cDNA encoding human and rat brain inositol polyphosphate 4-phosphatase. *J. Biol. Chem.* **270**, 16128-16133.

Norris, F. A., Atkins, R. C. and Majerus, P. W. (1997). The cDNA cloning and characterization of inositol polyphosphate 4-phosphatase type II. Evidence for conserved alternative splicing in the 4-phosphatase family. *J. Biol. Chem.* **272**, 23859-23864.

Odorizzi, G., Babst, M. and Emr, S. D. (2000). Phosphoinositide signaling and the regulation of membrane trafficking in yeast. *Trends Biochem. Sci.* **25**, 229-235.

Ory, D. S., Neugeboren, B. A. and Mulligan, R. C. (1996). A stable human-derived packaging cell line for production of high titer retrovirus/vesicular stomatitis virus G pseudotypes. *Proc. Natl. Acad. Sci USA* **93**, 11400-11406.

Paglin, S., Hollister, T., Delohery, T., Hackett, N., McMahill, M., Sphicas, E., Domingo, D. and Yahalom, J. (2001). A novel response of cancer cells to radiation involves autophagy and formation of acidic vesicles. *Cancer Res.* **61**, 439-444.

Panaretou, C., Domin, J., Cockcroft, S. and Waterfield, M. D. (1997). Characterization of p150, an adaptor protein for the human phosphatidylinositol (PtdIns) 3-kinase. Substrate presentation by phosphatidylinositol transfer protein to the p150.Ptdins 3-kinase complex. *J. Biol. Chem.* **272**, 2477-2485.

Paul, C. P., Good, P. D., Winer, I. and Engelke, D. R. (2002). Effective expression of small interfering RNA in human cells. *Nat. Biotechnol.* **20**, 505-508.

Petiot, A., Ogier-Denis, E., Blommaart, E. F., Meijer, A. J. and Codogno, P. (2000). Distinct classes of phosphatidylinositol 3′-kinases are involved in signaling pathways that control macroautophagy in HT-29 cells. *J. Biol. Chem.* **275**, 992-998.

Petiot, A., Faure, J., Stenmark, H. and Gruenberg, J. (2003). PI3P signaling regulates receptor sorting but not transport in the endosomal pathway. *J. Cell Biol.* **162**, 971-979.

Pohlmann, R., Boeker, M. W. and von Figura, K. (1995). The two mannose 6-phosphate receptors transport distinct complements of lysosomal proteins. *J. Biol. Chem.* **270**, 27311-27318.

Press, B., Feng, Y., Hoflack, B. and Wandinger-Ness, A. (1998). Mutant Rab7 causes the accumulation of cathepsin D and cation-independent mannose 6-phosphate receptor in an early endocytic compartment. *J. Cell Biol.* **140**, 1075-1089.

Prior, I. A. and Clague, M. J. (1999). Localization of a class II phosphatidylinositol 3-kinase, PI3KC2alpha, to clathrin-coated vesicles. *Mol. Cell. Biol. Res. Commun.* **1**, 162-166.

Reilly, J. J., Jr, Mason, R. W., Chen, P., Joseph, L. J., Sukhatme, V. P., Yee, R. and Chapman, H. A., Jr (1989). Synthesis and processing of cathepsin L, an elastase, by human alveolar macrophages. *Biochem. J.* **257**, 493-498.

Rijnboutt, S., Stoorvogel, W., Geuze, H. J. and Strous, G. J. (1992). Identification of subcellular compartments involved in biosynthetic processing of cathepsin D. *J. Biol. Chem.* **267**, 15665-15672.

Roggo, L., Bernard, V., Kovacs, A. L., Rose, A. M., Savoy, F., Zetka, M., Wymann, M. P. and Muller, F. (2002). Membrane transport in Caenorhabditis elegans: an essential role for VPS34 at the nuclear membrane. *EMBO J.* **21**, 1673-1683.

Row, P. E., Reaves, B. J., Domin, J., Luzio, J. P. and Davidson, H. W. (2001). Overexpression of a rat kinase-deficient phosphoinositide 3-kinase, Vps34p, inhibits cathepsin D maturation. *Biochem. J.* **353**, 655-661.

Sbrissa, D., Ikonomov, O. C. and Shisheva, A. (1999). PIKfyve, a mammalian ortholog of yeast Fab1p lipid kinase, synthesizes 5-phosphoinositides. Effect of insulin. *J. Biol. Chem.* **274**, 21589-21597.

Schu, P. V., Takegawa, K., Fry, M. J., Stack, J. H., Waterfield, M. D. and Emr, S. D. (1993). Phosphatidylinositol 3-kinase encoded by yeast VPS34 gene essential for protein sorting. *Science* **260**, 88-91.

Shin, H. W., Hayashi, M., Christoforidis, S., Lacas-Gervais, S., Hoepfner, S., Wenk, M. R., Modregger, J., Uttenweiler-Joseph, S., Wilm, M., Nystuen, A. et al. (2005). An enzymatic cascade of Rab5 effectors regulates phosphoinositide turnover in the endocytic pathway. *J. Cell Biol.* **170**, 607-618.

Siddhanta, U., McIlroy, J., Shah, A., Zhang, Y. and Backer, J. M. (1998). Distinct roles for the p110alpha and hVPS34 phosphatidylinositol 3′- kinases in vesicular trafficking, regulation of the actin cytoskeleton, and mitogenesis. *J. Cell Biol.* **143**, 1647-1659.

Simonsen, A., Lippe, R., Christoforidis, S., Gaullier, J. M., Brech, A., Callaghan, J., Toh, B. H., Murphy, C., Zerial, M. and Stenmark, H. (1998). EEA1 links PI(3)K function to Rab5 regulation of endosome fusion. *Nature* **394**, 494-498.

Simonsen, A., Wurmser, A. E., Emr, S. D. and Stenmark, H. (2001). The role of phosphoinositides in membrane transport. *Curr. Opin. Cell Biol.* **13**, 485-492.

Song, X., Xu, W., Zhang, A., Huang, G., Liang, X., Virbasius, J. V., Czech, M. P. and Zhou, G. W. (2001). Phox homology domains specifically bind phosphatidylinositol phosphates. *Biochemistry* **40**, 8940-8944.

Stack, J. H., DeWald, D. B., Takegawa, K. and Emr, S. D. (1995). Vesicle-mediated protein transport: regulatory interactions between the Vps15 protein kinase and the Vps34 PtdIns 3-kinase essential for protein sorting to the vacuole in yeast. *J. Cell Biol.* **129**, 321-334.

Stein, M. P., Feng, Y., Cooper, K. L., Welford, A. M. and Wandinger-Ness, A. (2003). Human VPS34 and p150 are Rab7 interacting partners. *Traffic* **4**, 754-771.

Sui, G., Soohoo, C., Affar, e. B., Gay, F., Shi, Y., Forrester, W. C. and Shi, Y. (2002). A DNA vector-based RNAi technology to suppress gene expression in mammalian cells. *Proc. Natl. Acad. Sci. USA* **99**, 5515-5520.

Traganos, F. and Darzynkiewicz, Z. (1994). Lysosomal proton pump activity: supravital cell staining with acridine orange differentiates leukocyte subpopulations. *Methods Cell Biol.* **41**, 185-194.

Vanhaesebroeck, B., Leevers, S. J., Ahmadi, K., Timms, J., Katso, R., Driscoll, P. C., Woscholski, R., Parker, P. J. and Waterfield, M. D. (2001). Synthesis and function of 3-phosphorylated inositol lipids. *Annu. Rev. Biochem.* **70**, 535-602.

Virbasius, J. V., Guilherme, A. and Czech, M. P. (1996). Mouse p170 is a novel phosphatidylinositol 3-kinase containing a C2 domain. *J. Biol. Chem.* **271**, 13304-13307.

Whitley, P., Reaves, B. J., Hashimoto, M., Riley, A. M., Potter, B. V. and Holman, G. D. (2003). Identification of mammalian Vps24p as an effector of phosphatidylinositol 3,5-bisphosphate-dependent endosome compartmentalization. *J. Biol. Chem.* **278**, 38786-38795.

Wiley, H. S. and Burke, P. M. (2001). Regulation of receptor tyrosine kinase signaling by endocytic trafficking. *Traffic* **2**, 12-18.

Wilson, A. L., Erdman, R. A. and Maltese, W. A. (1996). Association of Rab1B with GDP-dissociation inhibitor (GDI) is required for recycling but not initial membrane targeting of the Rab protein. *J. Biol. Chem.* **271**, 10932-10940.

Wilson, A. L., Erdman, R. A., Castellano, F. and Maltese, W. A. (1998). Prenylation of Rab8 GTPase by type I and type II geranylgeranyl transferases. *Biochem. J.* **333**, 497-504.

Wurmser, A. E. and Emr, S. D. (2002). Novel PtdIns(3)P-binding protein Etf1 functions as an effector of the Vps34 PtdIns 3-kinase in autophagy. *J. Cell Biol.* **158**, 761-772.

Wurmser, A. E., Gary, J. D. and Emr, S. D. (1999). Phosphoinositide 3-kinases and their FYVE domain-containing effectors as regulators of vacuolar/lysosomal membrane trafficking pathways. *J. Biol. Chem.* **274**, 9129-9132.

Xu, Y., Hortsman, H., Seet, L., Wong, S. H. and Hong, W. (2001). SNX3 regulates endosomal function through its PX-domain-mediated interaction with PtdIns(3)P. *Nat. Cell Biol.* **3**, 658-666.